

## Application of a Novel h-Shaped Ultrasonic Particle Separator under Microgravity Conditions

PACS REFERENCE: 43.35.Zc

Böhm<sup>1</sup>, H; Briarty<sup>1</sup>, LG; Lowe<sup>1</sup>, KC; Power<sup>1</sup>, JB; Benes<sup>2</sup>, E; Davey<sup>1</sup>, MR

<sup>1</sup>Plant Science Division, School of Biosciences, University of Nottingham

Sutton Bonington Campus, Loughborough LE12 5RD, UK; telephone: (+44)-115-951-3057; fax: (+44)-115-951-6334

<sup>2</sup>Vienna University of Technology, Institute of General Physics

Wiedner Hauptstrasse 8 – 10, A-1040 Vienna, Austria.

### ABSTRACT:

The application is described of a novel, h-shaped ultrasonic resonator for the separation of biological particulates. The effectiveness of the h-shaped resonator has been demonstrated using suspensions of the cyanobacterium, *Spirulina platensis*. Separation of *Spirulina* at cleared flow rates from 14 – 58 L/d, as assessed by remote video recording, was evaluated under both microgravity ( $\leq 0.05$  g) and terrestrial gravity conditions. In comparison with previous systems, the h-shaped resonator provided a more homogeneous acoustic field intensity, flow characteristics and overall separation efficiency ( $\sigma = 1$ , ratio of concentration in cleared phase to input), monitored with a turbidity sensor. The new separation concept also works in the absence of gravity forces, although gravity forces influenced overall efficiency. During a typical microgravity period of ca. 22 s, achieved during the 29<sup>th</sup> ESA Parabolic Flight Campaign,  $\sigma$  was  $0.96 \pm 0.01$  at a flow rate of 14 L/d, compared to terrestrial gravity conditions, whereas with increased flow rates (38 L/d),  $\sigma$  reduced to  $0.71 \pm 0.01$ . Overall, these results demonstrate that, for optimum resonator performance under the relatively short microgravity period utilised in this study, flow rates of ca. 14 L/d are preferable. These data provide a baseline for exploiting non-invasive, compact, ultrasonic separation systems for manipulating biological particulates under microgravity conditions.

Keywords: acoustic separation; cell trapping; microgravity, separation efficiency; *Spirulina platensis*; ultrasonic h-resonator

### INTRODUCTION

When exposed to an ultrasonic standing wave field, suspended microparticles are subjected to acoustic radiation forces, which cause the particles to migrate into the pressure nodal or antinodal planes of the sound field (King, 1934; Yosioka and Kawasima, 1955; Gor'kov, 1962; Nyborg, 1967; Crum, 1971; Gould and Coakley, 1974). Lateral and secondary acoustic forces, in turn, induce particles to form compact associates (Weiser and Apfel, 1984; Whitworth and Coakley, 1992). As a consequence, sedimentation of the cell associates is considerably accelerated. This effect is employed by sedimentation-based ultrasonic separation systems. The latter, and other ultrasonic separation systems (Apfel, 1990; Coakley et al. 1994; Coakley 1997; Gröschl, 1998a,b; Gröschl et al. 1998), are gaining increasing use over conventional mechanical separation systems, since acoustic separation systems are also free of mechanical flow barriers and are not susceptible to fouling. A further advantage of ultrasonic separation systems is

their ease of sterilisation, and general reliability of automated, electronically controlled operation.

Currently, ultrasonic separation systems have a range of biotechnological applications (Hawkes and Coakley, 1996; Bierau et al. 1998; Gröschl et al. 1998). A key application is in so-called acoustically enhanced sedimentation systems in combination with bio-reactors of the perfusion type (Gröschl et al. 1998). A promising flow-through separation concept based on a micro-chamber has been developed by Hawkes et al. (1998a,b) showing a comparatively high separation performance by exploiting the velocity gradient of the laminar flow profile in the chamber. More recently, an h-shaped resonator (Institute of General Physics, Vienna University of Technology, Vienna, Austria) has been developed that represents a significant improvement over earlier flow-through separation systems, e.g. the Y-shaped resonator (Frank et al. 1993; Trampler, 2000), since both sound field homogeneity and flow guiding geometry have been optimised (Benes, Atlanta, 2001). Advantageously, the micro-chamber, the Y-shaped and h-shaped separation concepts are gravitation-independent and, therefore, are expected to surpass sedimentation-based systems if suspensions with low particle/fluid mass-density contrast need to be separated and when separation in microgravity is required. In the present experiments, the ability of the h-shaped resonator to separate biological particles was investigated using cells of the cyanobacterium *Spirulina platensis*. The rationale for using *Spirulina* as the assay organism was based on the MELiSSA (Micro-Ecological Life Support Alternative) Final Report for 1999 (Lasseur and Fedele, 2000) managed by ESA/ESTEC, in which it was noted that micro-organisms such as *Spirulina* (Whitton and Potts, 2000) could be exploited to degrade waste products in future biological life support systems for long-term, manned space missions.

## MATERIALS AND METHODS

### Characteristics of the h-shaped resonator and experimental configuration

An ultrasonic microparticle filter of the type h-resonator (Institute of General Physics, Vienna University of Technology, Austria) was used as a cell separation unit (Figure 1). The acoustic force field was established by a plane standing wave field and cell suspensions were separated into a cleared (reduced cell concentration) and an enriched phase (increased cell concentration). The electric power supply was provided by high-frequency power generator (AGC, Biosep ADI 1015, Applikon Dependable Instruments B.V., Schiedam, The Netherlands). The throughput of the cell suspension was maintained and controlled by a peristaltic pump (Type 505; Watson-Marlow, Falmouth, UK). Pulsation dampers (balloons, 5 cm in diameter) reduced the variations of the input flow velocity (Figure 2).

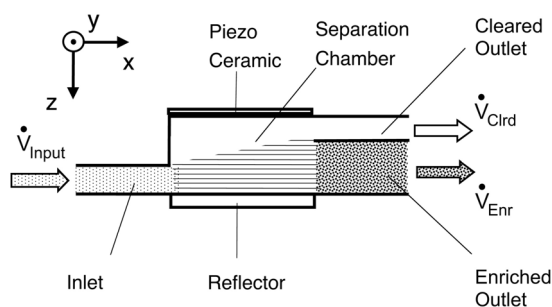


**Figure 1.** Schematic diagram of the h-shaped resonator.

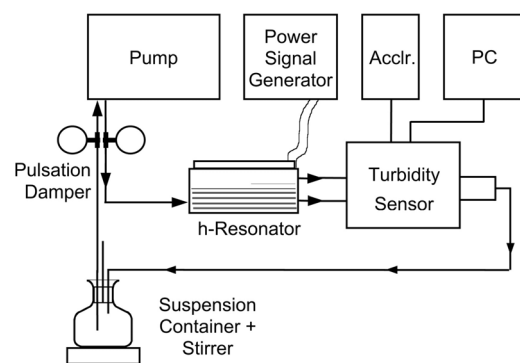


**Figure 2.** Arrangement of the h-shaped resonator and associated instrumentation.

A turbidity sensor (Hawkes et al. 2001) was employed to detect the optical backscatter signal of the suspension in phase, which was directly proportional to the cell density. The cleared and enriched phases were combined (and stirred) in a 500 ml plastic bottle reservoir (Nalgene, Rochester, NY, USA). Microgravity was attained aboard an Airbus A300 aircraft during the 29th ESA Parabolic Flight Campaign (November 21–24, 2000) in Bordeaux, France. A typical gravity sequence, including ca. 20 s of microgravity, is shown in Figure 3. Gravity was measured by an

accelerometer (SFIM Industries, Massy Cedex, France) and both the turbidity and acceleration data were recorded by a laptop PC at a time resolution of 3 sets of data points per second.

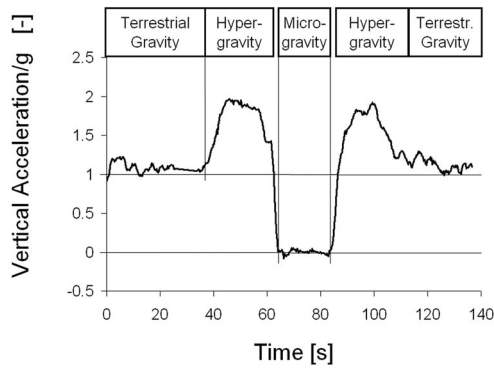


**Figure 3.** Typical vertical acceleration measured during one microgravity cycle.

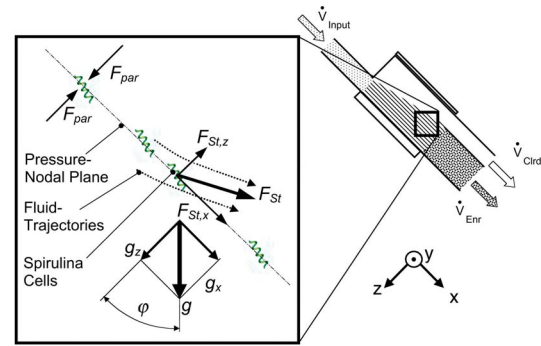


**Figure 4.** The h-shaped resonator in the operational position. The insert represents the axial primary acoustic radiation forces  $F_{par}$ , Stokes' forces  $F_{St}$  and gravity  $g$ , to which cells are exposed.

### Suspensions

Fixed (glutaraldehyde treated) cells of *Spirulina platensis* were used at a cell concentration adjusted to  $1.16 \times 10^5$  ml<sup>-1</sup> with culture medium. The dimensions of *Spirulina* cells were obtained by light microscopy.

### Separation process

Cells were subjected to 3 types of forces; ultrasound-induced acoustic forces (King, 1934; Yosioka and Kawasima, 1955; Gor'kov, 1962; Nyborg, 1967), shear (Stokes') forces and gravitational forces. Acoustic forces are induced by a standing wave field: The axial component of the primary acoustic radiation forces ( $F_{par}$ ) parallel to the  $z$ -direction of the co-ordinates (Figures 1, 4) accelerates the cells towards the pressure nodal planes of the standing wave field while their lateral components (not shown) in the  $x$ - $y$  plane (Figures 1, 4) drive the cells within the pressure-nodal planes towards areas of local maximum acoustic intensity. In ultrasonic separation systems, cells are subjected to acoustic and buoyancy forces (gravity). The resulting different trajectories and speeds of fluid and cells induce shear forces  $F_{St}$  (Figure 4).

The success of the separation process was quantified as

$$\sigma = 1 - \frac{n_{Clrd}}{n_{Input}} = \frac{I_{Input}^{sctr} - I_{Clrd}^{sctr}}{I_{Input}^{sctr} - I_0^{sctr}} \quad (1)$$

with  $n_{input}$  and  $n_{clrd}$  being the cell concentrations in the input duct and in the cleared outlet, respectively. As the relative change of the scatter signal  $I^{sctr}$  is proportional to the cell concentration  $n$  in the cleared outlet stream,  $\sigma$  can be calculated from the scatter signals with  $I_{Input}^{sctr}$  and  $I_{Input}^{sctr}$  being the signals of the input stream and the perfectly cell-cleared suspension, respectively.  $\sigma$  ranged from 0 to 1, the former representing the input cell concentration retained at the outlets, the latter indicating an ideal case of an entirely cell-free phase at the cleared outlet.

$\sigma$  was determined at cleared flow rate values of 14, 23, 38 and 58 L/d at an output flow ratio cleared/enriched of ca. 0.5. The resonator was positioned inclined at  $-45^\circ$  against the horizontal (Figure 4) and the transducer was operated at a series resonance frequency of about 1.95 MHz. An effective electrical input power of 4 Wrms was chosen.

### Statistical Methods

Means and standard errors (S E) were used throughout, as appropriate. Statistical significance between mean values was assessed, using conventional ANOVA and Student's  $t$  test

(Snedecor and Cochran, 1989). A probability of  $P < 0.05$  was considered significant.

## RESULTS

### Characteristics of *Spirulina* cell suspensions

The *Spirulina* suspension consisted of both straight and helical-shaped cells (Figure 6), the latter on average ( $\pm$  standard deviation,  $n = 10$ ) contributing to  $45 \pm 4$  % of the cell population. The mean length of the straight cells was  $170 \pm 85$   $\mu\text{m}$  ( $n = 216$ ), with a typical diameter of  $6 \pm 1$   $\mu\text{m}$  ( $n = 15$ ). Curved cells had a mean length of  $82 \pm 30$   $\mu\text{m}$  ( $n = 95$ ). Their mean outer diameter was  $31 \pm 6$   $\mu\text{m}$ , with a strand diameter of  $7 \pm 1$   $\mu\text{m}$  ( $n = 95$ ). *Spirulina* cells were generally separated as single cells in suspension. However, they tended to form loose aggregates.

### Separation of *Spirulina* cells under microgravity

Figure 5 shows the gravity and  $\sigma$  curves for the flow rates 14 to 58 L/d, both as a function of time. At pt. (a), the mean ( $\pm$  standard deviation,  $n = 3$ )  $\sigma$  values of  $0.98 \pm 0.01$ ,  $0.89 \pm 0.04$ ,  $0.79 \pm 0.08$  and  $0.52 \pm 0.07$  were obtained with flow rates of 14, 23, 38 and 58 L/d, respectively. While microgravity conditions only minimally decreased mean  $\sigma$  to  $0.96 \pm 0.01$  at 14 L/d,  $\sigma$  declined to  $0.77 \pm 0.07$  and  $0.71 \pm 0.08$  at 23 and 38 L/d, respectively. At a cleared flow rate of 58 L/d,  $\sigma$  decreased to a lesser extent, reaching a value of  $0.55 \pm 0.02$ .

Examples of frames from video recordings of the separation process during the parabolic cycles are shown in Figures 6 and 7. Generally, a stable separation pattern in the re-resonator chamber was attained at 13, 11, 9 and 7 s following the transition from hyper-gravity to microgravity conditions, when cleared flow rates of 14, 23, 38 and 58 L/d, respectively, were applied. Figures 6 and 7 show the separation patterns characterised by the local cell distributions in the resonator chamber; the pts. (a) and (c) in the subsections a to d, represent terrestrial gravity and micro-gravity, respectively (compare with Fig. 5). Flow rates of 14 and 38 L/d are compared in Figures 6 and 7. At the minimum cleared flow rate evaluated (14 L/d),

the cell separation pattern was unaffected by gravity. Axial acoustic forces retained most cells in the pressure nodal planes concentrating the cells in the lower third of the chamber, and the residual upper part of the volume remained clear. At a cleared flow rate of 38 L/d, separation was impaired, as illustrated by an example shown in Figure 7. At 1 g (a), the cell-enriched phase in the lower part of the chamber volume was not as clearly detached from the uppermost cell-cleared phase as it was at a lower flow rate. Cells were removed from the pressure nodal planes by Stokes' forces and increasingly streamed towards the cleared outlet. Under micro-gravity conditions, more cells were removed from the planes, resulting in steeper cell trajectories. Interestingly, during hypergravity, such trajectories flattened and the marked wedge-shaped, cell-rich phase observed previously did not occur.

Figure 6a shows the undesirable influence of lateral acoustic forces on the separation pattern at a low flow rate (14L/d), with cells being trapped in three columns. Such columns generated by lateral ( $x$ ,  $y$ -directions) variations of the displacement-amplitude distribution. At higher flow rates (38 L/d) the columns were comparably less pronounced (Figure 7a).

## DISCUSSION

Overall, the present study has demonstrated the effectiveness of the novel h-resonator for the separation of biological particulates, specifically those of *S. platensis*. The key advantages of this separation concept, compared to acoustically-enhanced sedimentation systems, are that its functionality is not restricted to both the presence of gravity and a different mass density of the fluid phase and particulates. Compared to previously described Y-shaped systems (Curtis and

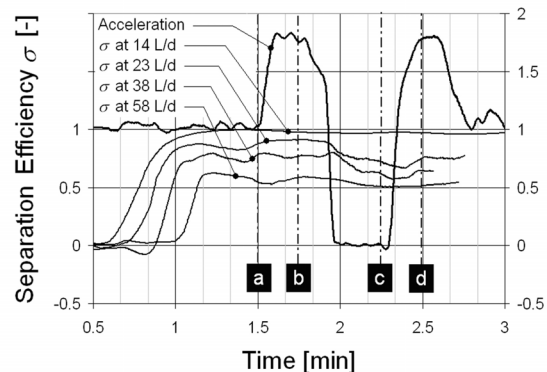


**Figure 5.** Mean  $\sigma$  for cleared flow rates (left y-axis) of 14, 23, 38 and 58 L/d, as well as the vertical acceleration in multiples of g (right y-axis), as functions of time ( $n = 3$  throughout).

Stephans, 1982; Frank et al. 1993), the present approach also demonstrates improved field quality and flow characteristics. Collectively, such features lead to a significant increase in operability, reliability and, crucially, optimum flow rate. Thus, the new separation approach has potentially wider applications in biotechnology, including downstream processing and perfusion systems for bioreactors. One key outcome from the present experiments under microgravity was that, at a low cleared flow rate (i.e. 14 L/d),  $\sigma$  was unchanged compared to terrestrial gravity conditions. Despite the good separation achieved with the novel resonator, one limitation was cell trapping caused by lateral components of the primary acoustic radiation forces. Related studies (Whitworth and Coakley, 1992; Böhm et al. 2001) suggested that cell trapping occurring as a result of acoustic forces obviously can be reduced when the lateral sound field intensity distribution is more homogeneous.

In this study, whilst good separation was achieved, the efficiency of the process was limited by the removal of cells from the pressure nodal planes caused by non-parallel trajectories of cells and fluid. Different  $z$ -components of the velocity vectors create shear forces, which may exceed the  $z$ -component of the primary acoustic radiation force. This, in turn, forces cells out of the pressure nodal planes. Such acoustic forces cannot be arbitrarily increased without the risk of reducing cell viability (Böhm et al. 2000) or causing cavitation (Giordano et al. 1976; Miller 1986).

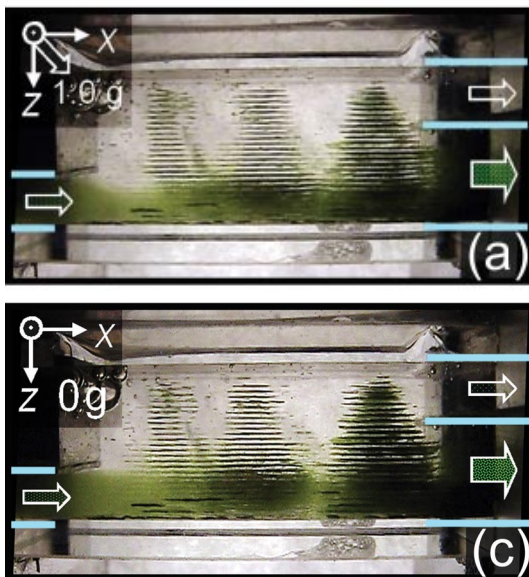


**Figure 6.** Separation pattern in the chamber of the h-shaped resonator at a cleared flow rate of 14 L/d at (top to bottom) 1 g (a) and 0 g (c, below). Co-ordinates represent orientation of the system. Gravity vector indicates amount and direction of vertical acceleration. Horizontal arrows represent input (left), output (right) from the separation chamber.

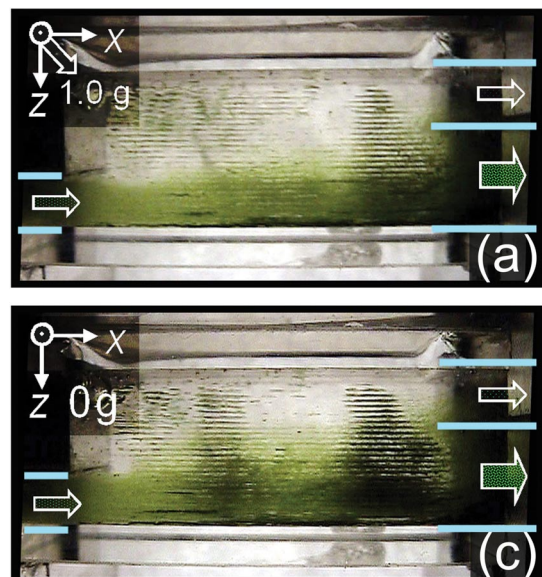


**Figure 7.** Separation pattern in the chamber at a cleared flow rate of 38 L/d at 1 g (a), and 0 g (c, below). Arrows as in Figure 6.

Therefore, one approach for reducing such shear forces is to decrease the relative velocity in the  $z$ -direction. Such forces can also be minimised by introducing a second ultrasonic standing wave field propagating in the  $y$ -direction, thereby moving cells into lines parallel to the  $x$ -axis. Consequently, this would increase gaps between adjacent lines (of cells), thereby reducing shear forces. Overall, the results from the present study demonstrate that, for optimum resonator performance under the relatively short microgravity period utilised in this investigation, flow rates of typically 14 L/d are preferred. Whilst it is recognised that additional experimentation is required to identify factors influencing cell separation in longer-term microgravity experiments, the present investigation provides a baseline for exploiting non-invasive, compact, ultrasonic separation systems to manipulate biological materials under microgravity conditions. Such technology, once optimised, will be valuable in operating biophysical processes, including life support systems, during space exploration.

## ACKNOWLEDGEMENTS

Work supported by the European Commission's TMR Programme EuroUltraSonoSep, Contract No. ERBFMRXCT97-0156.

## REFERENCES

- Apfel RE. 1990. Acoustic radiation pressure – Principles and application to separation science. Proceedings of the Fortschritte der Akustik – DAGA '90 Conference. Teil A. Bad Honnef: DPG-GmbH. p 19-36.
- Benes E, M. Gröschl, H. Nowotny, F. Trampler, T. Keijzer, H. Böhm, S. Radel, L. Gherardini, J.J. Hawkes, R. König, Ch. Delouvroy, 1990. Ultrasonic Separation of Suspended Particles, Invited Review Paper. Proc. of the 2001 IEEE International Ultrasonics Symposium, a Joint Meeting with the World Congress on Ultrasonics, Atlanta, Georgia, USA, Oct. 7-10, 2001, pp 649-659.
- Bierau H, Perani A, Al-Rubeai M, Emery AN. 1998. A comparison of intensive cell culture bioreactors operating with hybridomas modified for inhibited apoptotic response. J Biotechnol 62:195-207.
- Böhm H, Anthony P, Davey MR, Briarty LG, Power JB, Lowe KC, Benes E, Gröschl M. 2000. Viability of plant cell suspensions exposed to homogeneous ultrasonic fields of different energy density and wave type. Ultrasonics 38:629-632.
- Böhm H, Trampler F, Briarty LG, Lowe KC, Power JB, Benes E, Davey MR. 2001. Lateral displacement amplitude distribution of water-filled ultrasonic bio-separation resonators with laser-interferometry and thermochromatic foils. Proceedings of the 12<sup>th</sup> IEEE International Symposium on the Application of Ferroelectrics. p 725-728.
- Coakley WT. 1997. Ultrasonic separations in analytical biotechnology. Trends Biotechnol 15:506-511.
- Coakley WT, Whitworth G, Grundy MA, Gould RK, Allman R. 1994. Ultrasonic manipulation of particles and cells. Bioseparation 4:73-83.
- Crum LA. 1971. Acoustic force on a liquid droplet in an acoustic stationary wave. J Acoust Soc Am 50:157-163.
- Curtis HW, Stephans EJ. 1982. Ultrasonic continuous flow plasmapheresis separator. IBM Technical Disclosure Bulletin 25:192-193.
- Frank A, Bolek W, Gröschl M, Burger W, Benes E. 1993. Separation of suspended particles by use of the inclined resonator concept. Proceedings of the Ultrasonics International '93 Conference. Oxford: Butterworth-Heinemann. p 519-522.
- Giordano R, Leuzzi U. 1976. Effects of ultrasound on unicellular algae. J Acoust Soc Am 60:275.
- Gor'kov LP. 1962. On the forces acting on a small particle in an acoustical field in an ideal fluid. Sov Phys Dokl 6:773-775.
- Gould RK, Coakley WT. 1974. The effects of acoustic forces on small particles in suspension. Proceedings of the Symposium on Finite-Amplitude Wave Effects in Fluids 1973. Guildford: Pergamon Press. p 252-257.
- Gröschl M. 1998a. Ultrasonic separation of suspended particles - Part I: Fundamentals. Acustica 84:432.
- Gröschl M. 1998b. Ultrasonic separation of suspended particles - Part II: Design and operation of separation devices. Acustica 84:632.
- Gröschl M, Burger W, Handl B, Doblhoff-Dier O, Gaida T, Schmatz C. 1998. Ultrasonic separation of suspended particles - Part III: Application in biotechnology. Acustica 84:815.
- Hawkes JJ, Coakley WT. 1996. A continuous flow ultrasonic cell filtering method. Enzyme Microbial Tech 19:57-62.
- Hawkes JJ, Barrow D, Coakley WT. 1998a. Microparticle manipulation in millimetre scale ultrasonic standing wave chambers. Ultrasonics 36, 925-931.
- Hawkes JJ, Barrow D, Cefai J, Coakley WT. 1998b. A laminar flow expansion chamber facilitating downstream manipulation of particles concentrated using an ultrasonic wave. Ultrasonics 36:901-903.
- Hawkes JJ, Coakley WT. 2001. Force field particle filter, combining ultrasound standing waves and laminar flow. Sensor Actuat B-Chem 75:213-222.
- Hawkes JJ, Gröschl M, Nowotny H, Armstrong S, Tasker PJ, Coakley WT, Benes E. 2001. Single half wavelength ultrasonic particle filter: Predictions of the transfer matrix multi-layer resonator model and experimental filtration results. J Acoust Soc Am (Submitted).
- King LV. 1934. On the acoustic radiation pressure on spheres. Proc R Soc London A147:212-240.
- Lasseur C, Fedele I, editors. 2000. MELiSSA Final Report for 1999, ESA/EWP-2092, The Netherlands.
- Miller DL. 1986. Effects of high-amplitude 1-MHz standing ultrasonic field on the algae *hydrodictyon*. IEEE Transactions on Ultrasonics, ferroelectrics and frequency control. UFFC-33 2:165-170.
- Nyborg WL. 1967. Radiation pressure on a small rigid sphere. J Acoust Soc Am 42:947-952.
- Snedecor GW, Cochran WG. 1989. Statistical methods, 8<sup>th</sup> edition. Ames: Iowa State College Press.
- Weiser MAH, Apfel RE. 1984. Interparticle forces on red cells in a standing wave field. Acustica 56:114-119.
- Whitton BA, Potts A. 2000. The ecology of cyanobacteria – Their diversity in time and space. Dordrecht: Kluwer Academic Publishers.
- Whitworth G, Coakley WT. 1992. Particle column formation in a stationary ultrasonic field. J Acoust Soc Am 91:79-85.
- Yosioka K, Kawasima Y. 1955. Acoustic radiation pressure on a compressible sphere. Acustica 5:167-173.